Lab on a Chip

Accepted Manuscript

ROYAL SOCIETY OF CHEMISTRY

www.rsc.org/loc

Table of Content Entry

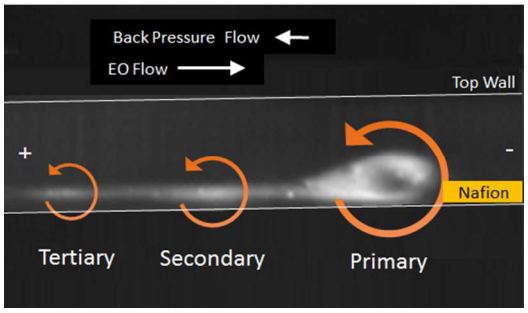

Primary, secondary and tertiary vortex **generated inside an ion concentration polarization (ICP) region all rotating in the same direction.**

Vortex Chain Formation in Regions of Ion Concentration Polarization

Srinivas Hanasoge, Francisco J. Diez
Rutgers, The State University of New Jersey

Abstract:
The local vortical flow generated inside an ion concentration polarization (ICP) region is evaluated experimentally. The ICP is induced by a patterned nano-porous self-assembling membrane integrated inside a single micro channel. A bottom-view image of the depletion region near the membrane revealed a primary vortex which results from the electric field amplification. A unique perspective of the flow is obtained by imaging the microchannel from its side. This visualization shows for the first time the formation of a chain of three vortices all rotating in the same direction in the depletion region. While observation of multiple vortices has been previously reported, it was in reference to counter rotating vortex pairs and not to a same direction of rotation vortex chain formation. A physical model is proposed which considers a two dimensionally varying concentration profile in the depletion region to account for the formation of multiple vortices rotating in the same direction. The fast rotating primary vortex changes the local concentration in regions adjacent to it, as the advection time scale is much higher than the diffusion time scale. Near the membrane, it moves low concentration electrolyte from the bottom wall upwards into higher concentration region. Away from the membrane, it moves high concentration electrolyte from the middle of the channel downwards into a low concentration region. These local changes in the wall concentration result in a varying slip velocity capable of inducing a secondary vortex. Similarly, this secondary vortex can induce a tertiary one. A numerical simulation is performed using the proposed varying slip velocity model which showed an excellent agreement with the experimental observations.

Introduction:
Ion transport at nano-scale has gained increased importance as rapid advances in nano-fabrication techniques enables novel fluid manipulation methods. For channel dimensions approaching the Debye length scale, the electric double layer from opposing walls will overlap resulting in an excess counter-ion concentration in the channel. When an electric field is applied, different electro-migration rates for the counter ions and co ions (selective permeability) can lead to the depletion of ions on one side and enrichment of ions on the other side of a nano-channel. This phenomenon of charge redistribution (ion concentration polarization, ICP) across a nano-channel has been widely considered in the literature.[1–6]

Recent measurements including flow visualizations in nano-channels and membranes have increased our understanding of the ICP phenomena [7–10]. These studies lead to various techniques for fluid handling and manipulation in Lab-on-chip devices such as the application of nano-porous membranes in water desalination and other filtering techniques[11]. They also lead to applications including pre-concentration techniques[12,13] and micro-scale mixing[14,15]. A detailed review on the application of ICP for pumping, mixing, pH actuation, analyte concentration among others can be found in Slouka et al[16].

The depletion of electrolyte in the ICP leads to pre-concentration or stacking of ionic species [8,12,17,18]. For instance, Bharadwaj & Santiago[17] showed how the stacking of analytes across a low concentration buffer region leads to field amplified sample stacking. A similar effect, termed ion pre-concentration, has been observed in regions of concentration polarization[8,12].

A hydrodynamic effect that has been observed in the depletion region is the formation of vortices. These can form due to different physical phenomena. For instance, in electrokinetics of the second kind, the formation of an extended space charge near the surface of an ion-selective membrane leads to electric field focusing and hence the formation of a pair of counter rotating vortex along the plane of the chip substrates[19–22]. Other studies have reported the formation of pair of counter rotating vortices near a conductor with finite permittivity of the electric field[23,24]. Other similar phenomenon observed near sharp corners due to field leakage[25,26] and changes in local pH[27] results in non-uniform zeta potential, thereby affecting the local hydrodynamics.

The formation of vortices in ICP devices has application in enhancing pre-concentration and mixing. This work describes a same direction of rotation vortex chain formation in the ICP, which was experimentally observed in a single channel pre-concentrator. We first describe the setup involving a patterned nano-porous self-assembling membrane integrated inside a single micro channel. Next, imaging of the depletion region shows the vortex chain. This is followed by a discussion about the concentration distribution, velocity field, and wall slip velocity necessary to generate a primary vortex in the depletion region. Then, a physical model is proposed which considers a two dimensionally varying concentration profile. Next, we describe how the mixing from primary vortex induces changes in the wall slip velocity inducing a secondary vortex. This can then generate a tertiary vortex and so on. Finally, a simulation is performed to validate the physical model.

Experimental Setup

The experimental setup consists of a nano-porous self-assembling membrane integrated inside a micro channel. The fabrication method is discussed in detail by Kim et al.[28] and uses flow patterning and soft lithography. Briefly, a Nafion 117 solution (Sigma Aldrich) is patterned on the glass substrate using a reversibly bonded micro channel (50µm width x 20µm thickness). The micro channel is then removed and the patterned Nafion is cured at 80^{o}C for 10 minutes. The cured Nafion forms a self-assembled nano-porous membrane with a pore size of around 5nm. A PDMS micro-channel is then bonded to this glass slide, in a direction perpendicular to the patterned membrane, using oxygen plasma. *Figure 1* shows a sketch of the microfluidic device. It should be noted that the nano-porous membrane occupies only a small section of the bottom wall of the microchannel as highlighted in the inset in Fig. 1. We performed experiments with various rectangular micro-channels ranging from 50µm to 300µm in width. The thicknesses of the channels used were 20µm to 50µm.

The macro reservoirs used for sample entry and exit are mm-size holes punched into the PDMS. When an electric field is applied across the two reservoirs, we see an overall electro-osmotically driven flow in the device from the anode to the cathode, along with effects of concentration polarization near the membrane. The microfluidic device is mounted in an inverted Nikon Eclipse Ti microscope. Videos are captured, both along the plane of the substrate and perpendicular to the substrate, using a Rolera Mgi camera and a 10x objective. All experiments are performed with a DC bias applied across the reservoirs using platinum electrodes. Negatively charged b-phycoerythrin dye is used to observe the concentration variations in the channel. Nano-colloids, 1 micron in diameter (Life Technologies) are used to observe the flow characteristics. Both are used in a 0.01mM phosphate buffer solution (pH=7.5). The electro-osmotic flow is dominant, and hence the electrophoretic mobility of the colloids is not considered in the analysis[29–32].

Results:

When a DC voltage bias is applied across the device, it results in a depletion of ions on the anodic side of the membrane. The formation of the depletion region is confirmed by monitoring the fluorescent intensity of b-Phycoerythrin dye which decreases when the voltage is applied. In the current configuration, there is a depletion region on the anodic side but not an enrichment region on the cathodic side of the nano-porous membrane as the bulk electro-osmotic flow drives away any enrichment of ions all the way to the reservoir.

For this microfluidic configuration, there are two main effects related to the ion depletion. These are field amplified sample stacking, FASS, and the generation of micro vortices. Briefly, stacking of the negatively charged fluorescent dye is observed on the anodic side of the depletion region (pre-concentration/ FASS). The ion species are redistributed by their electro-migration rate differences, as the electric field is amplified across the depletion region. While stacking occurs for the negative ions, it does not occur for the positive ions, as the electro osmotic flow drives them away to the reservoir. This is confirmed by tracing a positive dye, Rhodamine G6 (Sigma Aldrich), which showed no sample stacking.

The second effect is the formation of micro vortices in the depletion region. These are visualized experimentally by seeding the flow with nano-colloids and tracking their motion in the region adjacent to the nafion membrane. The flow visualization in a plane along the chip substrate shows and oscillatory back and forth motion of the nano-colloids (see supplemental video 1). This oscillatory motion is the projection of a vortex in that plane and it is similar to the observations by Yossifon & Chang[33]. While this bottom-view visualization provides evidence of a vortex, additional hydrodynamic flow details are needed. In order to get information such as the direction of motion and size of the vortex, side-view images of the channel are taken by placing the chip on its side. This allowed capturing images perpendicular to the glass substrate (along the side wall). This view reveals the formation of the primary vortex along with the depletion region (Supplemental Video 3) and a chain of three vortices (Fig. 2) all rotating in the same direction as shown by the supplemental video 2. The videos and Fig. 2 shows a primary vortex with a tear drop shape while the two smaller vortices are elongated in the direction of the flow.

This new evidence of the formation of a secondary and tertiary vortex obtained from the side-view images in Fig. 2 could be considered similar to those observed by Kim et al.[28] that used a bottom-view approach. However, upon closer inspection (see supplemental video 2), these vortices are not the counter-rotating vortices seen by those authors, instead the video shows that they all rotate in the same direction which has not been previously reported. This suggest that the driving mechanism is different from others reviewed in the literature such as electrokinetics of the second kind and ICEO flow. Vortices due to electro-osmosis of the second kind form along a plane perpendicular to the ones observed in these experiments. They are in a plane along the bottom wall[22,33]. Also, the observed phenomenon cannot be due to induced charge electro-osmosis (ICEO) either, as that generates a pair of counter-rotating vortices. This is due to the polarization of the membrane which would result in non-uniform zeta potential and therefore an ejecting flow over the membrane surface[23,25,26]. Moreover, unlike the observed vortices in our experiments, these vortices are in a plane parallel to the bottom wall. Last, ion depletion leading to slip velocity variation and formation vortices has also been reported by several authors[26,34,35]. For instance, in Takhistov et al.[26] the high permittivity corner induces the depletion

instead of the currently used nafion membrane. The vorticity direction is consistent with a slip-velocity mechanism, where it is perpendicular to the net electro-osmotic flow direction.

Next, we propose a physical model capable of generating multiple vortices that rotate in the same direction in the depletion region. The dynamics of the model reflects how the primary vortex induces the secondary vortex, and this secondary vortex induces a tertiary vortex and so on.

Discussion:

Vortex Formation Model:

We propose a physical model where the formation of multiple chain micro vortices is the result of a non-uniform electro-osmotic velocity in the depletion region. Before expanding on this physical model we will review single vortex formation process. Briefly, as the anodic side of the membrane gets depleted, there is a local increase in the electric field strength which increases the electro-osmotic slip velocity. This accelerated flow along the bottom wall drives the formation of the primary vortex. Since the nafion membrane is patterned on the bottom wall, the depletion region effects are dominant on that wall and not the top wall.

Typically, the ion concentration polarization for a nano-porous membrane can be explained with a 1D model[36]. To understand the formation of the primary vortex, let us first assume the membrane to be not interacting with the electric field (Zero electricity permittivity). For the present configuration, with the membrane patterned on the bottom wall, this 1D model would only be applicable along the bottom wall. (We propose a more realistic model, with a finite membrane permittivity, in the next section to accommodate for these assumptions). Such a model yields a linear ionic concentration decrease along the bottom wall of the depletion region[37] notionally sketched in Fig. 3a. Similarly, the electric potential and electric field in this region, sketched in Fig. 3b, will be non-uniform as predicted by Yossifon et al.[36] and Kim et al.[4]. Considering that the electro-osmotic slip velocity is proportional to the local electric field, we expect the slipping velocity to also show a similar non-uniform behavior resulting in an accelerated flow along the channels' bottom wall (notionally sketched in *Fig. 3c*). In this closed-system, as the flow is accelerated along the bottom wall a reverse flow is needed to satisfy conservation of mass in the channel. This combination leads to the formation of the vortex.

A numerical simulation is used to show that these flow conditions generate a single vortex. The flow in the microchannel is modeled in COMSOL and the slip velocity from Fig 3c is used as the bottom wall boundary condition. The simulation shows that for this closed-cell type system, the electro-osmotic flow drives the fluid near the wall towards the cathode, and the built up pressure drives the fluid in the center of the channel towards the anode during steady state. Furthermore, the analysis demonstrates the formation of the vortex along the bottom wall as shown by the velocity streamlines and velocity vector field in Fig. 4. These numerical results are in good agreement with the experimental results in Fig. 2 and demonstrate that the slip velocity variations along the wall lead to the vortex formation. It is important to note that the maximum fluid velocity reached in the depletion region can be as high as 20~30 times the bulk velocity[28]. This renders the flow in the depletion region convection dominated (High Péclet number).

2D Concentration Polarization Effects

In the previous physical model, however, we did not consider the finite permittivity of the membrane and the effects of the primary vortex on the local hydrodynamics. We only considered the depletion region spreading in the x-direction along the bottom wall. In reality, however, due to the finite thickness and conductivity of the membrane the electric field lines are not parallel but rather curved and directed into the membrane as shown in Fig. 5. If we apply the previous ion depletion discussion to this electric field geometry one would expect a two-dimensionally varying concentration field in the x- and y-direction moving away from the membrane as shown in Fig. 5. This brings up the question of how would this change the 1D model previously discussed. Also, would the fast moving vortex observed in the depletion region affect this two-dimensionally varying concentration field? These will be address next.

The primary vortex sketched in Fig. 5 suggests that its fast rotating motion will affect the local concentration in two regions. It is important to note that at the velocity scale of the primary vortex, the Péclet number is high (>100). This means that the diffusive mixing is slow as compared to convective mixing, implying the primary vortex is essentially folding the fluid[38,39]. Near the membrane, the vortex moves low concentration electrolyte from the bottom wall upwards into the middle of the channel's higher concentration region. Away from the membrane, the vortex forces high concentration electrolyte from the middle of the channel downwards into the bottom wall low concentration region. Overtime this vortex eliminates the concentration gradient and an eventual concentration plateau forms. A similar concentration plateau has been experimentally observed by Kim et al.[28] (in their Fig. 4a). There is a sudden change in concentration between this plateau (primary vortex region) and the rest of the depletion region as shown in Fig. 6a (similar to Kim et al[28]). This leads to a non-uniform change in the electric potential (figure 6b), affecting the local velocity field. The fluid in this region is therefore accelerated, leading to the formation of the secondary vortex. The secondary vortex induces the tertiary, and so on. The slip velocity in the depletion region is therefore expected to have a step like profile as seen depicted in Figure 6c.

A numerical simulation is performed to test the physical model proposed. This further helps visualizing the hydrodynamic behavior of the fluid in the depletion region. For this simulation, the lower wall boundary condition is modeled using the varying slip velocity from *Fig. 7a*. The simulation demonstrates the formation along the bottom wall of the three vortices all rotating in the same direction. This is shown by the velocity streamlines and velocity vector field in Fig. 7b. These numerical results are in good agreement with the measurements in Fig. 2 and even reproduce the elongated tear drop shape of the vortex observed in the experiments. The simulation further shows that the varying slip velocity along the wall generates fluid flow that leads to the vortex motion.

Conclusion:

We evaluated the vortical flow that develops in the ICP region near a patterned nano-porous self-assembling membrane integrated inside a single micro channel. Imaging the microchannel from its side, provided a unique perspective about the depletion region in this flow. The side-view images reveal the formation of a chain of three vortices all rotating in the same direction. This differs from previous

observations in the literature where counter rotating vortex pairs have been described from bottom-view images. Our results suggest that a more complete and accurate picture about the hydrodynamics of the flow is available when combining bottom-view imaging and side-view imaging.

We proposed a physical model that explains the formation in the depletion region of three micro vortices rotating in the same direction. These are the result of a non-uniform slip velocity. Briefly, as the depletion region forms so does the primary vortex as shown by the starting vortex video. This vortex changes the local concentration in regions adjacent to it. Near the membrane, the vortex moves low concentration electrolyte from the bottom wall upwards into the middle of the channel's higher concentration region. Away from the membrane, the vortex forces high concentration electrolyte from the middle of the channel downwards into the bottom wall low concentration region. These local changes in the wall concentration can accelerate or decelerate the slip velocity which induces a secondary vortex. Similarly this secondary vortex can induce a tertiary one. This model is validated with a numerical simulation that matched the experimental results showing excellent agreement.

A key feature in the proposed model was the presence of a two dimensionally varying concentration field in the depletion region. Further studies should be carried out to thoroughly compute this concentration field as well as the induced varying slip velocity by the vortices. This is essential to better understand the mixing behavior of these vortices, and to show their capabilities in enhancing pre-concentration in ICP devices. Last, they can also have applications in particle extraction and separation.

References:

1 D. Hlushkou, R. Dhopeshwarkar, R. M. Crooks and U. Tallarek, *Lab. Chip*, 2008, **8**, 1153.
2 I. Vlassiouk, S. Smirnov and Z. Siwy, *Nano Lett.*, 2008, **8**, 1978–1985.
3 Q. Pu, J. Yun, H. Temkin and S. Liu, *Nano Lett.*, 2004, **4**, 1099–1103.
4 S. J. Kim, L. D. Li and J. Han, *Langmuir*, 2009, **25**, 7759–7765.
5 H.-C. Chang and G. Yossifon, *Biomicrofluidics*, 2009, **3**, 012001.
6 G. Yossifon, P. Mushenheim, Y.-C. Chang and H.-C. Chang, *Phys. Rev. E*, 2009, **79**.
7 S. J. Kim, Y.-C. Wang, J. H. Lee, H. Jang and J. Han, *Phys. Rev. Lett.*, 2007, **99**.
8 J. H. Lee, Y.-A. Song and J. Han, *Lab. Chip*, 2008, **8**, 596.
9 R. Dhopeshwarkar, L. Sun and R. M. Crooks, *Lab. Chip*, 2005, **5**, 1148.
10 R. Dhopeshwarkar, R. M. Crooks, D. Hlushkou and U. Tallarek, *Anal. Chem.*, 2008, **80**, 1039–1048.
11 S. J. Kim, S. H. Ko, K. H. Kang and J. Han, *Nat. Nanotechnol.*, 2010, **5**, 297–301.
12 S. H. Ko, Y.-A. Song, S. J. Kim, M. Kim, J. Han and K. H. Kang, *Lab. Chip*, 2012, **12**, 4472.
13 Y.-C. Wang, A. L. Stevens and J. Han, *Anal. Chem.*, 2005, **77**, 4293–4299.
14 H. Jeon, H. Lee, K. H. Kang and G. Lim, *Sci. Rep.*, 2013, **3**.
15 E. Choi, K. Kwon, S. J. Lee, D. Kim and J. Park, *Lab Chip*, 2015, **15**, 1794–1798.
16 Z. Slouka, S. Senapati and H.-C. Chang, *Annu. Rev. Anal. Chem.*, 2014, **7**, 317–335.
17 R. Bharadwaj and J. G. Santiago, *J. Fluid Mech.*, 2005, **543**, 57.
18 K. Zhou, M. L. Kovarik and S. C. Jacobson, *J. Am. Chem. Soc.*, 2008, **130**, 8614–8616.
19 I. Rubinstein and B. Zaltzman, *Phys. Rev. E*, 2010, **81**.
20 I. Rubinstein and B. Zaltzman, *Adv. Colloid Interface Sci.*, 2007, **134-135**, 190–200.
21 A. S. Khair, *Phys. Fluids*, 2011, **23**, 072003.
22 G. Yossifon and H.-C. Chang, *Phys. Rev. Lett.*, 2008, **101**.
23 T. M. Squires and M. Z. Bazant, *J. Fluid Mech.*, 2004, **509**, 217–252.

24 Y. Eckstein, G. Yossifon, A. Seifert and T. Miloh, *J. Colloid Interface Sci.*, 2009, **338**, 243–249.
25 S. K. Thamida and H.-C. Chang, *Phys. Fluids*, 2002, **14**, 4315.
26 P. Takhistov, K. Duginova and H.-C. Chang, *J. Colloid Interface Sci.*, 2003, **263**, 133–143.
27 A. R. Minerick, A. E. Ostafin and H.-C. Chang, *ELECTROPHORESIS*, 2002, **23**, 2165–2173.
28 S. J. Kim, S. H. Ko, R. Kwak, J. D. Posner, K. H. Kang and J. Han, *Nanoscale*, 2012, **4**, 7406.
29 R. J. Hunter, *Zeta Potential in Colloid Science: Principles and Applications*, Academic Press, 1981.
30 J. H. Masliyah and S. Bhattacharjee, *Electrokinetic and Colloid Transport Phenomena*, John Wiley & Sons, 2006.
31 P. H. Paul, M. G. Garguilo and D. J. Rakestraw, *Anal. Chem.*, 1998, **70**, 2459–2467.
32 M. Sureda, A. Miller and F. J. Diez, *ELECTROPHORESIS*, 2012, **33**, 2759–2768.
33 G. Yossifon and H.-C. Chang, *Phys. Rev. E*, 2010, **81**.
34 K.-D. Huang and R.-J. Yang, *Microfluid. Nanofluidics*, 2008, **5**, 631–638.
35 K.-D. Huang and R.-J. Yang, *ELECTROPHORESIS*, 2008, **29**, 4862–4870.
36 G. Yossifon, P. Mushenheim, Y.-C. Chang and H.-C. Chang, *Phys. Rev. E*, 2010, **81**.
37 S. J. Kim, Y.-A. Song and J. Han, *Chem. Soc. Rev.*, 2010, **39**, 912.
38 A. D. Stroock, S. K. Dertinger, A. Ajdari, I. Mezić, H. A. Stone and G. M. Whitesides, *Science*, 2002, **295**, 647–651.
39 C.-C. Chang and R.-J. Yang, *Microfluid. Nanofluidics*, 2007, **3**, 501–525.

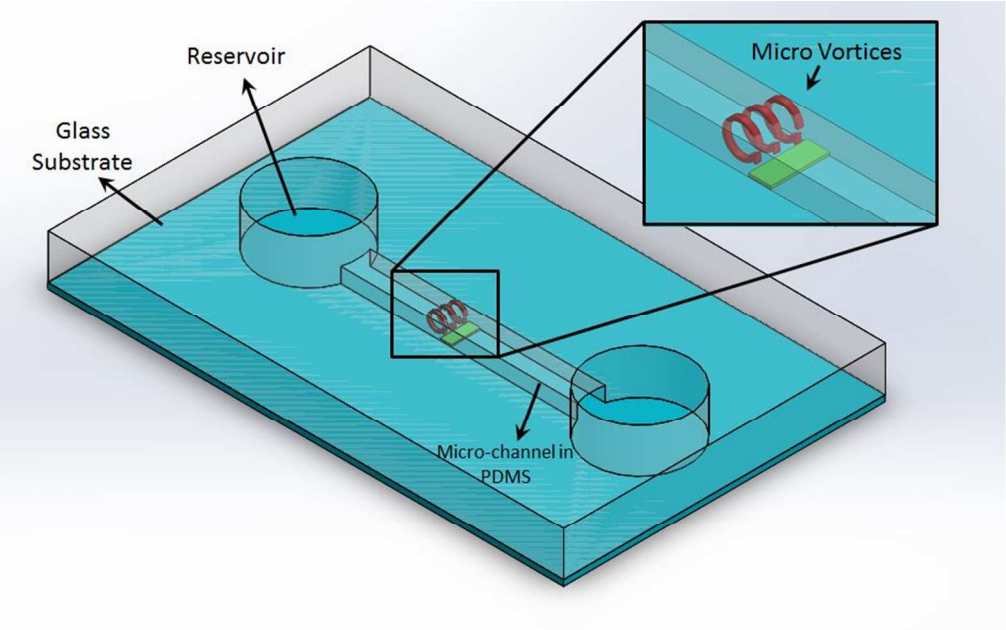

Figure 1: Sketch of the microfluidic system including the nafion membrane deposited in the bottom wall.

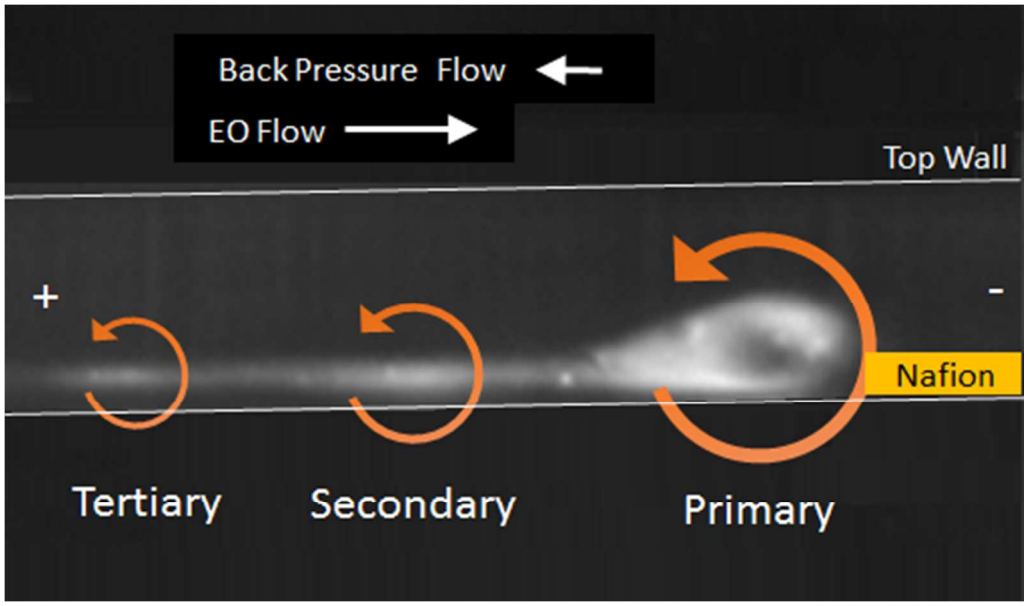

Figure 2: Side-view of the primary, secondary and tertiary vortex. The nafion membrane is approximately 5um in height in this 100 um tall channel and it is patterned only over the section marked. For further details showing that direction of rotation is the same for all three vortices see supplemental video 1.

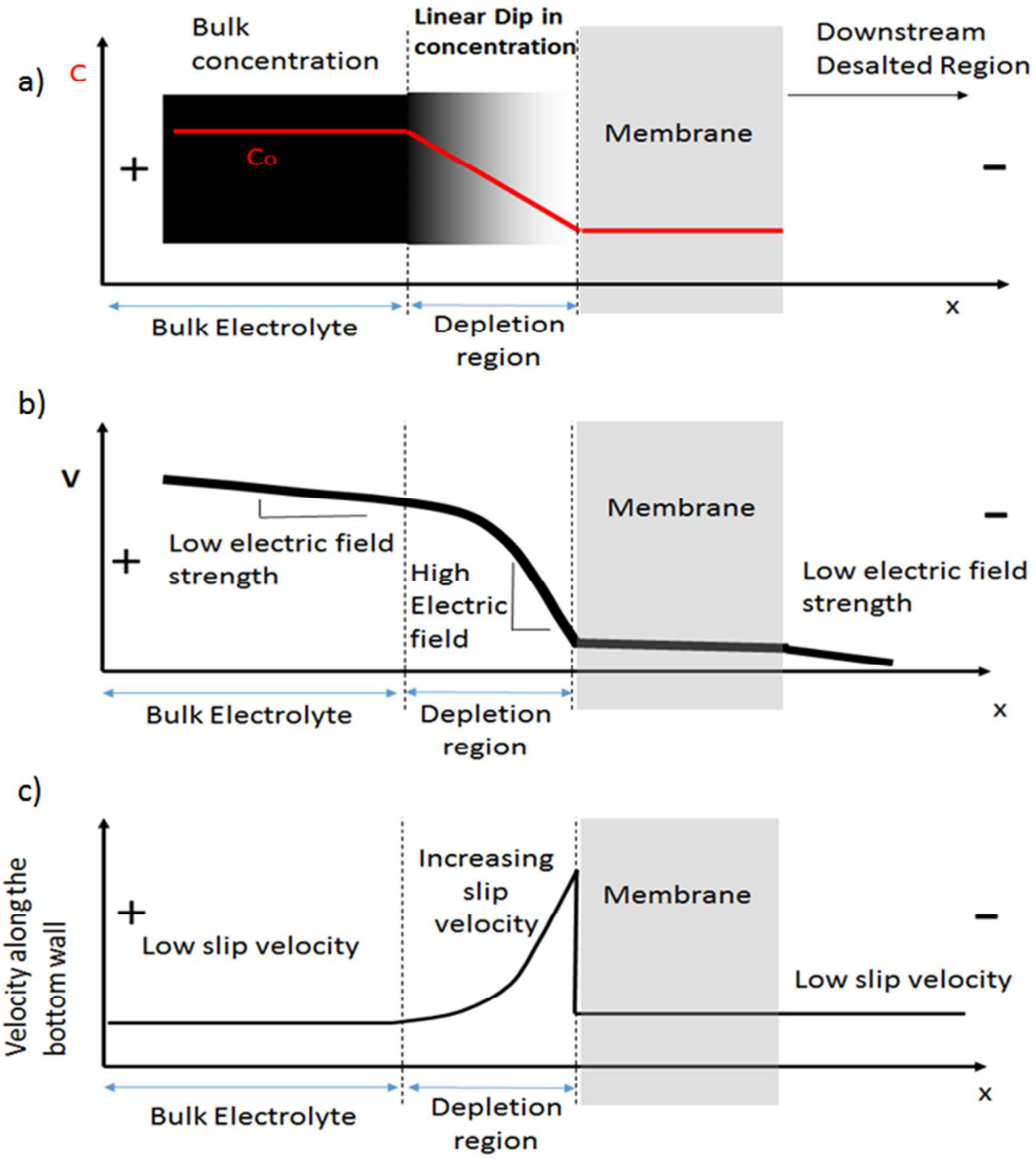

Figure 3: (a) Concentration variation along the bottom wall as predicted for a 1D membrane. (b) Electric potential along the channel, shows the variation due to a linear depletion region. (c) Slip velocity due to non-uniform electric field along the bottom wall. Details about the downstream region for nanofluidic channels can be found in Kim 2009.

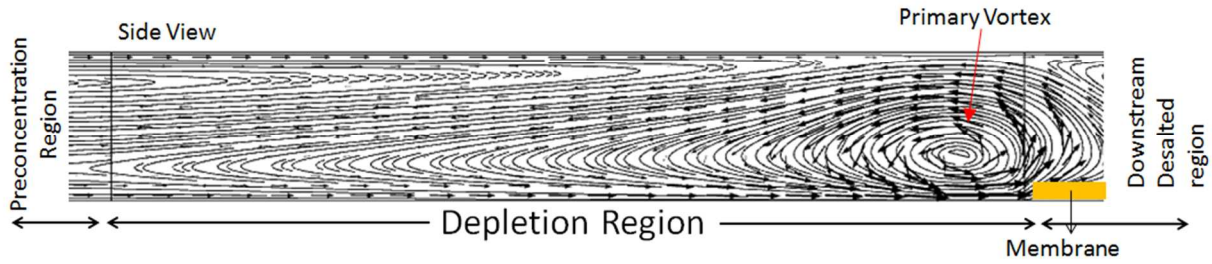

Fig. 4 Side-view image of the microchannel showing the calculated velocity streamlines from the numerical simulation. The primary vortex is induced by the accelerating flow near the bottom wall close to the nafion membrane (yellow).

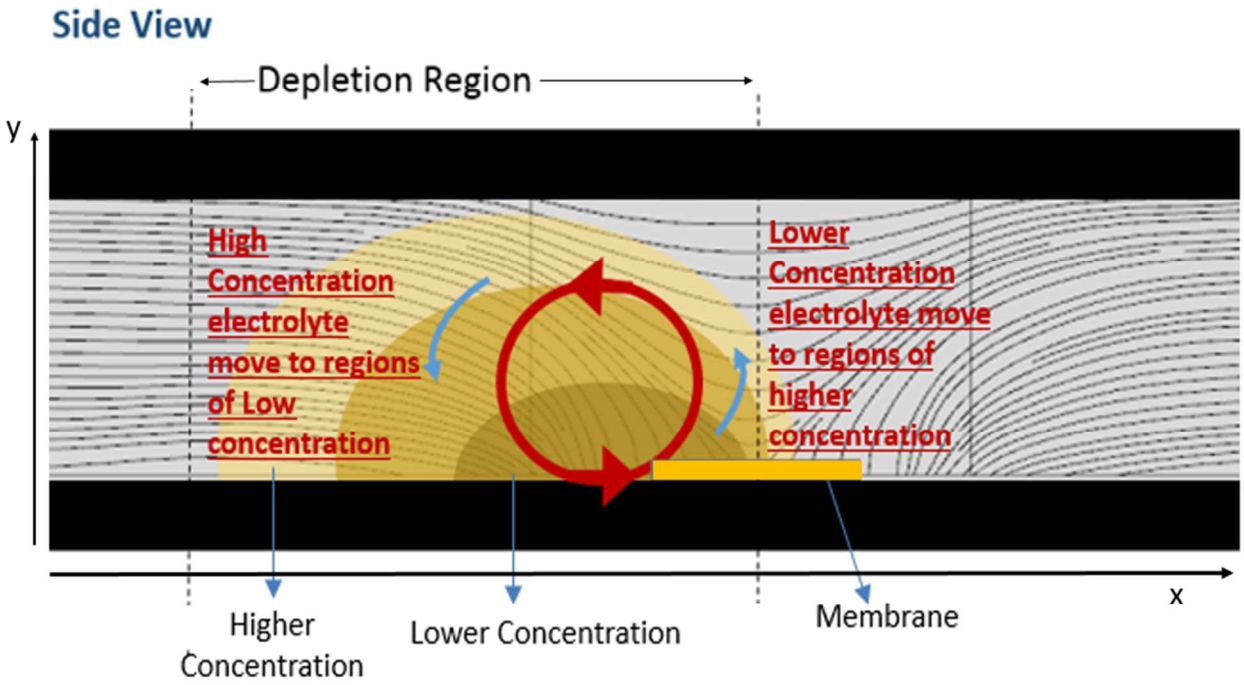

Figure 5: Side-view sketch of the microchannel showing the two-dimension variation of the concentration as well as the electric field lines. Finite conductivity of the membrane leads to electric field lines perpendicular to the membrane, thereby leading to a concentration that varies in the x- and y-directions.

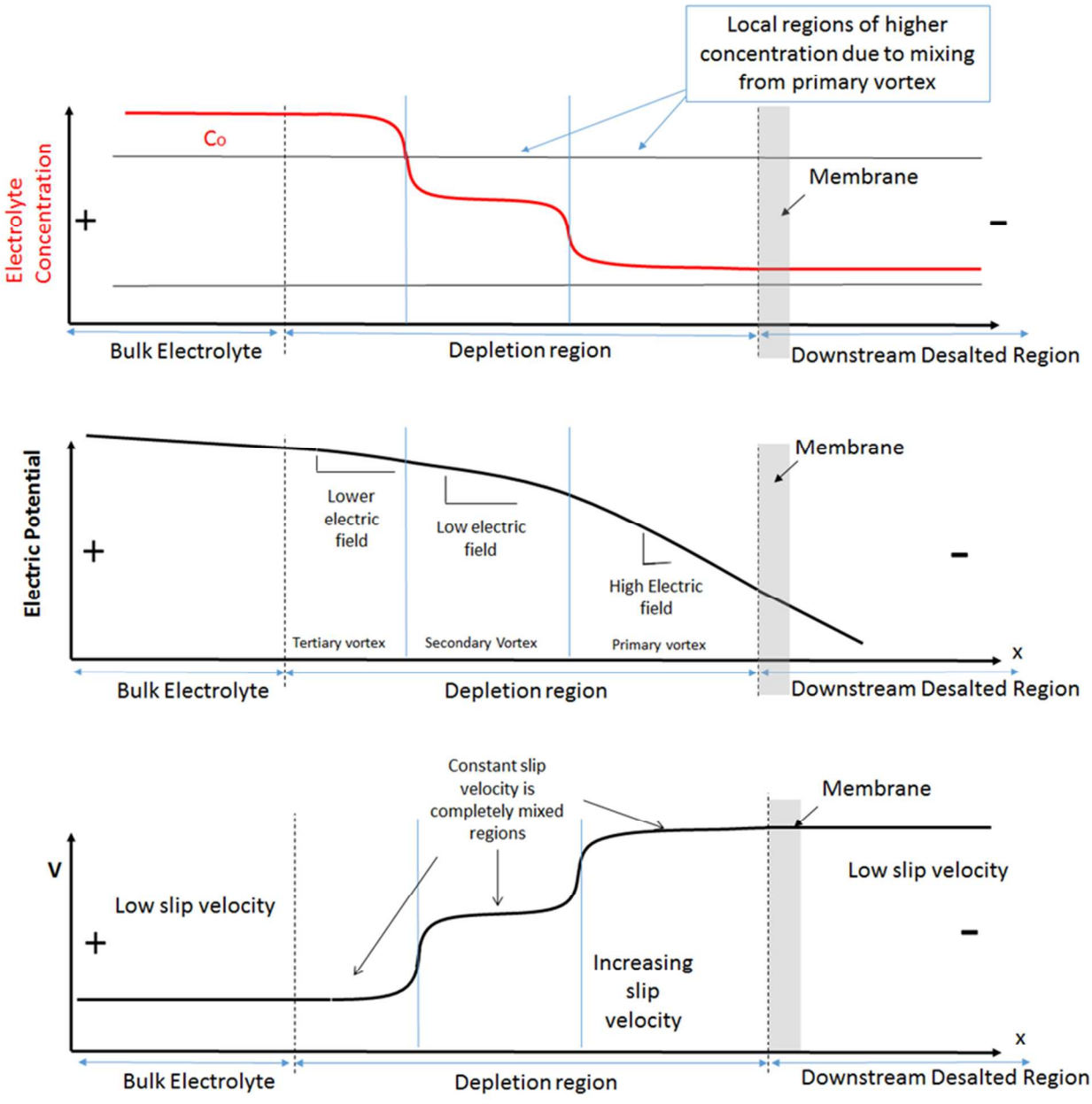

Figure 6: (a) Concentration along the bottom wall of the channel due to the mixing effect of the vortices. (b) Electric potential along the bottom. (c) Slip velocity along the bottom wall that shows the "bumps" due to the mixing effect of the vortices.

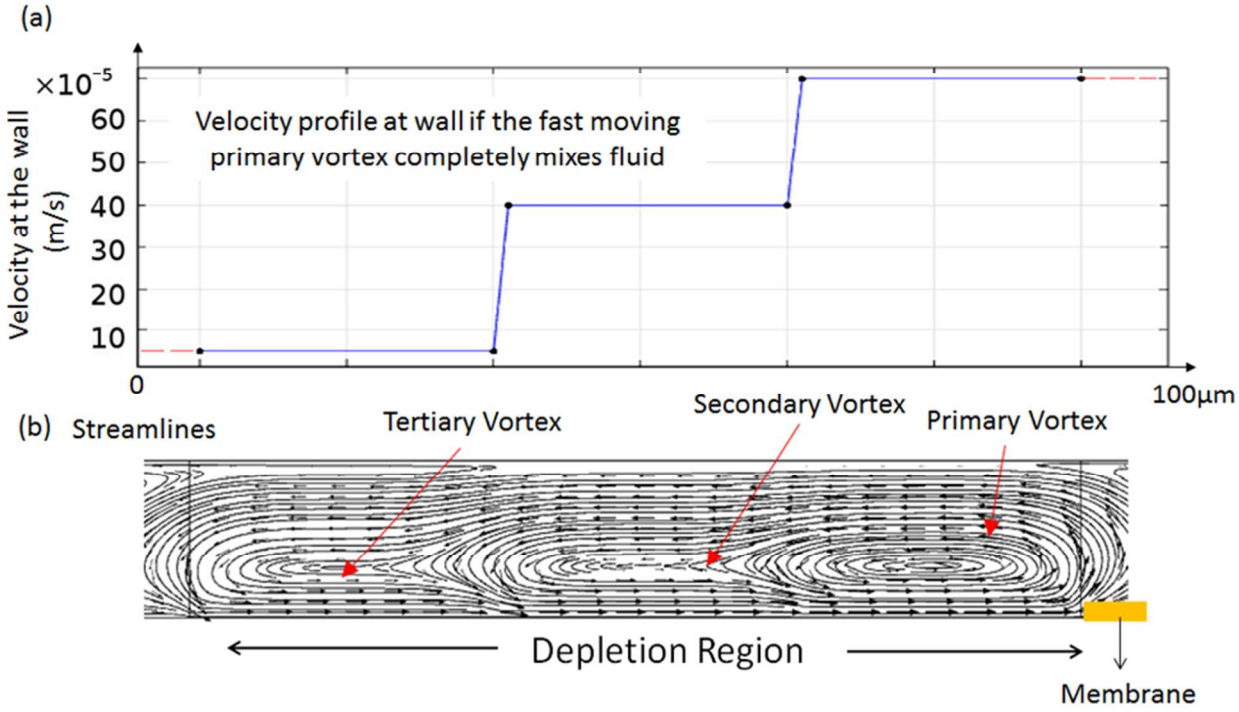

Figure 7: (a) Applied slip velocity boundary condition resulting from proposed model for generating multiple vortices. (b) Side-view image of the microchannel showing the calculated velocity streamlines from the numerical simulation. The primary, secondary and tertiary vortices all rotating in the same direction can be seen by the streamlines.